ISSN 2176-5480

22nd International Congress of Mechanical Engineering (COBEM 2013)
November 3-7, 2013, Ribeirão Preto, SP, Brazil

MODELING AND PARAMETER IDENTIFICATION OF A PNEUMATIC PRESSURE VALVE USING LEAST SQUARES AND PARTICLE SWARM OPTIMIZATION METHODS

Rodrigo Trentini
Leibniz Universität Hannover (LUH), Institut für Regelungstechnik (IRT), Hannover, Germany
preuss@irt.uni-hannover.de

Guilherme Espindola
Alexandre Campos
Antonio da Silva Silveira
Universidade do Estado de Santa Catarina (UDESC), Centro de Ciências Tecnológicas (CCT), Joinville, Brazil
espindola.gui@gmail.com
alexandre.campos@joinville.udesc.br
antonios@joinville.udesc.br

Abstract. *This paper presents the mathematical modeling and parameter identification of a pneumatic pressure valve. The applicability of pneumatic systems in industrial environments has become usual in the last years. Their main advantages are the low cost, maintenance simplicity and security, besides they are clean, renewables and abundant. However, their mainly disadvantages are the nonlinearities due to friction and air compressibility, which difficult their modeling and control. Proportional valves perform an important role in pneumatic control systems. Knowing their internal parameters, it is possible to increase the models reliability, since such parameters have significant influence in system dynamics. In this paper, the valve mathematical model is obtained through Mass and Energy Conservation Theory, where a piecewise sixth order linear model is obtained. Later, two sixth order piecewise black-box models using distinct parameters identification methods, being Least Squares and Particle Swarm Optimization, are reached. Testbed experiments show that the used valve has deadband and hysteresis, featuring a nonlinear plant. The unknown model constants determination is carried out through mathematical and black-box models comparison. A comparative analysis between both used identification methods is performed, where it is stated that Particle Swarm Optimization method is able to achieve smaller errors than Least Squares method for the proposed application.*

Keywords: *Parameter identification, Particle Swarm Optimization, Modeling of Pneumatic systems, .*

1. INTRODUCTION

It is well known that compressed air is one of the oldest forms of energy, but its application in industry took place only since 1950, where it replaced the human power in repetitive tasks. Nowadays, compressed air became indispensable in several industrial sections. Pneumatic systems work with high efficiency, performing repetitive operations, saving time, tools and materials. Furthermore, it is a renewable, clean, abundant and cheap energy form. Devices moved by compressed air have a high power/weight relation, low cost, maintenance facility and flexibility in installation. Currently, the main applications in pneumatic field are related to linear motion with final course stopping, among of cutting, drilling, thinning and finishing.

Lately, servopneumatics are being used when intermediate positions are required. These systems use actuators, electronic systems and control valves to reach high-end results. It is important to notice that servopneumatic applications reduce the air consumption by up to 30% in comparision to standard systems (Festo, 2010).

However, servopneumatic systems presents several difficulties in control, as air compressibility and friction effects. Such characteristics make the mathematical model more complex with the inclusion of nonlinear behaviour on it. Ali *et al.* (2009) state that friction is the major difficulty to obtain a satisfactory model. Pneumatic friction effects, like Coulomb, static, Stribeck and viscous, cause undesired effects as steady state and tracking errors, stick-slip movements and limit cycles around the desired position (Carneiro and Almeida, 2011).

Due to these drawbacks, electric systems are most commonly used in servopositioning systems than pneumatic ones, whereas accurate positions are not easily reached in pneumatics (Scholz and Zimmermann, 1993). Therefore, several researches aim to minimize the nonlinearities influence using different control strategies reaching accuracies up to 5 μm (Carneiro and Almeida, 2011).

Besides the friction problem, it is important to notice that an accurate valve model is required to improve computer simulations and control design in pneumatic systems. However, internal parts of pneumatic proportional valves are hardly

ISSN 2176-5480

known, so standard models are often used in simulations. Nevertheless, researches which aim to represent the dynamical behaviour of different control valves are being presented over the last years. For instance, Sorli *et al.* (2001) show a 2nd order nonlinear model of an ordinary proportional pressure valve using Mass and Energy Conservation Theory. Carneiro and Almeida (2006) present a proportional directional valve static model through artificial neural networks, reaching errors less than 5%. Taghizadeh *et al.* (2009) demonstrate a nonlinear dynamic model of a pneumatic fast switching valve to be used with PWM control applications. Additionally, some researchers as Guenther and Perondi (2004), Ritter (2010) and Barreto (2003) do not consider the dynamical features of pneumatic servovalves stating that their natural frequency are much higher than the natural frequency of the pneumatic actuator. It is worth highlighting that this consideration may be important aiming controllers design, where the goal is to obtain a reduced model that owns the main system features. Nevertheless, concerning to servopneumatic system simulations, the valve dynamic equationing plays an important role on its analysis.

In spite of the cited researches, the valve internal constants remain unidentified, since hardly ever the valve suppliers inform these parameters in their datasheets, which justifies the use of computational tools to address this issue. Hence, this paper presents a generic method for the parameter identification of a pneumatic proportional pressure valve using Least Squares (LS) and Particle Swarm Optimization (PSO) methods. A testbed is developed, where a pressure sensor, a data acquisition system and a proportional valve are used.

In this paper, the valve description is present in Section 2. The system mass conservation is analysed in Section 3, as well as its mass flow rate and forces balance. Section 4 shows the valve black-box identification using LS and PSO methods, whereas in Section 5 the internal parameter determination and identification methods comparison is carried out. The study conclusions are presented in Section 6.

2. VALVE DESCRIPTION

The manual proportional pressure regulator valves, or only *pressure valves*, are a specific case of pressure regulator valves. This kind of valve operates by the force balance principle, and the pressure regulation is carried out through a plunger in opposition to a spring force, spool displacement and internal pressure output (Dall'Amico, 2011). Curatolo *et al.* (2003) state that these valves operate regulating their output pressure at a value proportional to an input reference. A generic schematic drawing of a pressure valve is shown on Fig. 1. All of its internal components are considered with cylindrical shape.

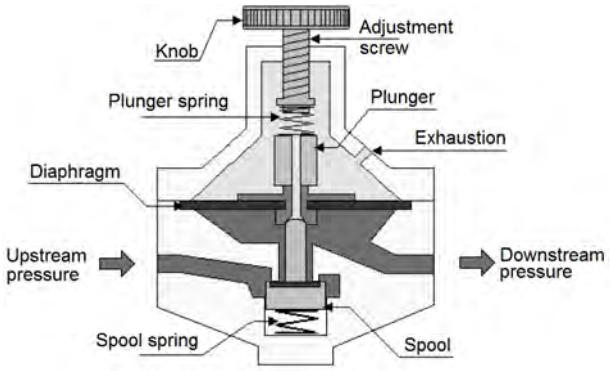

Figure 1. Manual generic pressure valve schematic drawing. Based on Curatolo *et al.* (2003).

The dark area on Fig. 1 shows the valve internal control volume. The plunger, which is separeted of the spool, has a leaked part where the pressure is relieved through the exhaustion port.

In order to understand the pressure valve operation, it is considered a null displacement on the adjustment screw, so that all the internal components are positioned as on Fig. 1. When a positive displacement on the adjustment screw happens, the plunger is displaced from top to bottom. If the produced force on the plunger spring is higher than the spool spring force, the spool, which at this moment is in contact with the plunger, moves downwards so that a upstream mass of air fills the control volume.

The air volume increment into the control volume increases the valve internal pressure. When the plunger spring force is lower than the force applied on the spool by the screw displacement itself, the input port is blocked. Hence, the pressure valve stays at the position shown on Fig. 1.

However, if the force due to the control volume pressure is higher than the force on the plunger spring, the valve diaphagm deforms itself upwards. Then, the spool reaches its mechanical limit and an air volume passes through the leaked plunger, exiting the valve through the exhaustion port until the force due to the control volume pressure and the force due to the plunger spring are the same, so that the components return to the position shown on Fig. 1.

An important feature of these kind of valves is the dead band on the beginning of their operation range, which may

ISSN 2176-5480

varies according to their internal components and manufacturers.

In next Section the mathematical modeling using Mass and Energy Conservation Theory of a generic pressure valve is present.

3. MATHEMATICAL MODEL

In mathematical modeling, it is often required to reach a trade off between model simplicity and accuracy, also called Principle of Parsimony. However, in many cases the simplifications are not easy to be done, and some *a priori* system knowledge is required, since if some relevant dynamics is neglect, the mathematical model may not have the needed accuracy. In this work the main used simplifications are:

- the compressed air kinetic energy is neglected;
- the environment and air temperature are constant;
- the air is a perfect gas;
- the specific pressure and volume heat are constant;
- there are no leakages;
- the system entropy is constant.

3.1 Mass conservation

Considering the cited simplifications, the equating proposed in this Section concerns to the Mass and Energy Conservation theory used for compressed fluids presented by Fox and McDonald (1985).

Being the control volume depicted by the dark area on Fig. 1, the system mass conservation indicates that the mass variation into the control volume is equal to the total mass flow that enter or exit throughout the control surface (Perondi, 2002), so:

$$\frac{\partial}{\partial t}\int_{VC}\rho\, dV \; + \int_{SC}\rho v\, dA_0 \; = 0 \tag{1}$$

where dV is the volume differential, v is the fluid speed, ρ is the density, A_0 is the control surface area and VC and SC are the control volume and surface, respectively.

Considering that the density is invariant with the volume, the first term on Eq. 1 become:

$$\frac{\partial}{\partial t}\int_{VC}\rho\, dV \; = \rho\frac{dV}{dt} + V\frac{d\rho}{dt} \tag{2}$$

By being a compressible fluid, ρ is function of pressure p and time t, or in other words, $\rho = f(p(t))$, therefore:

$$\rho\frac{dV}{dt} + V\frac{d\rho}{dt} = \rho\frac{dV}{dt} + V\frac{d\rho}{dp}\frac{dp}{dt} \tag{3}$$

The term $\rho\frac{dV}{dt}$ represents the control volume mass accumulation rate due to the volume variation itself, and the term $V\frac{d\rho}{dp}\frac{dp}{dt}$ represents the control volume mass accumulation due to the air compressibility (Perondi, 2002).

The second term of Eq. 1 corresponds to the liquid fluid flow rate, and it could be written considering the mass flow rate as:

$$\int_{SC}\rho v\, dA_0 \; = -\Delta q \tag{4}$$

where Δq is the liquid difference between the mass flow rates that enter and exit the system.

Therefore, replacing Eq. 3 and 4 in Eq. 1,

$$\Delta q = \rho\frac{dV}{dt} + V\frac{d\rho}{dp}\frac{dp}{dt} \tag{5}$$

being p the pressure into the valve control volume.

The air compressibility coefficient β at a constant temperature is given by the applied pressure rate and the volumetric rate of a given control volume ($\beta = -V dp/dV$) (Fox and McDonald, 1985), so:

$$\beta = \rho\frac{dp}{d\rho} \tag{6}$$

ISSN 2176-5480

Replacing Eq. 6 in Eq. 5:

$$\Delta q = \rho \frac{dV}{dt} + \frac{V\rho}{\beta}\frac{dp}{dt} \tag{7}$$

For perfect gases $\rho = p/(RT)$, where R is the universal gas constant and T is the absolute temperature. In addition, the compressibility coefficient for reversible adiabatic processes is $\beta = \gamma p$, being γ the rate between the gas specific heat for constant pressure and volume ($\gamma = C_p/C_v$). Then, neglecting the control volume variation, the mass flow rates for the control volume pressurization q_m and exhaustion q_e are given respectively by:

$$q_m = \frac{V}{\gamma RT}\dot{p} \tag{8}$$

$$q_e = \frac{V}{\gamma RT}\dot{p} \tag{9}$$

3.2 Mass flow rate

The mass flow rates given by Eq. 8 and 9 are analysed using the mass flow equating for compressible fluid shown by Fox and McDonald (1985). Some considerations are also taken into account:

- the process is adiabatic, reversible and has high speed, featuring an isentropic process;
- the flow is unidiretional;
- the fluid speed is uniform;
- the stagnation pressure p_{sup} is kept constant.

Generalizing, the valve input may be considered as a convergent nozzle. Therefore, according to Fox and McDonald (1985) there is a limit for the mass flow rate through the nozzle, featuring that the flow is blocked and mass flow rates at supersonic conditions are not reached.

Figure 2 shows the relation between the mass flow rate q with the absolute stagnation down- and upstream pressures — p_m and p_j respectively — in the pressure valve.

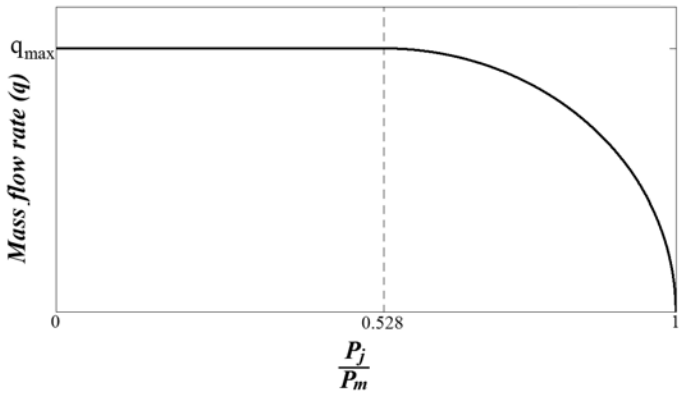

Figure 2. Relation between down- and upstream pressures with the mass flow rate for a compressible fluid through a nozzle. Based on Fox and McDonald (1985).

It is noted that from 52.8% of the upstream pressure p_m, the mass flow rate has nonlinear behavior. Therefore, taking into account only the linear range shown on Fig. 2, being the absolute supply pressure $p_{sup} = 8 \cdot 10^5$ Pa and the atmospheric pressure $p_{atm} = 1 \cdot 10^5$ Pa, the absolute pressure p_a into the control volume must be subjected to the restriction

$$1.894 \cdot 10^5 \text{ Pa } \leq p_a \leq 4.224 \cdot 10^5 \text{ Pa} \tag{10}$$

As the pressure valve operates with manometric pressure, the restriction become,

$$0.894 \cdot 10^5 \text{ Pa } \leq p \leq 3.224 \cdot 10^5 \text{ Pa .} \tag{11}$$

which represents the restriction that the pressure p must have so that the mass flow rate has linear feature.

ISSN 2176-5480

Hence, the expression which represents the blocked mass flow rate for a compressible fluid in a convergent nozzle is (Fox and McDonald, 1985):

$$q = Ap_m\sqrt{\frac{\gamma}{RT}\left(\frac{2}{\gamma+1}\right)^{\frac{\gamma+1}{\gamma-1}}} \tag{12}$$

where A is the control port area, which for the analised valve depends on the spool displacement when there is no mass flow rate through the exhaustion port. On the other hand, whenever there is mass flow rate through the exhaustion port, the area A depends only on the plunger displacement. Then, it may be state that:

$$A = k_1 x_c \text{ for } q_m \tag{13}$$
$$A = k_2 x_e \text{ for } q_e, \tag{14}$$

being x_c the spool displacement, x_e the plunger displacement, and k_1 and k_2 are proportionality constants between x_c and x_e and the analised control port cross-sectional area, respectively. Therefore, Eq. 12 may be written as:

$$q_m = k_1 k_a x_c p_{sup} \tag{15}$$
$$q_e = k_2 k_a x_e p \tag{16}$$

which are the final expressions for the mass flow rate, being q_m and q_e the flow rate for the valve pressurization and exhaustion, respectively, and $k_a = \sqrt{\frac{\gamma}{RT}\left(\frac{2}{\gamma+1}\right)^{\frac{\gamma+1}{\gamma-1}}}$.

3.3 Force balance

The force balance on the pressure valve is given by Newton's 2nd Law. However, there are two different situations that must be analised: whenever the control volume pressure p is lower than the regulated pressure p*, and whenever p is higher than p*. This is because, whenever $p > p$* the spool displacement is mechanically limited, so that, at this situation, its dynamics does not influence the system pressure. These conditions indicates the air flow direction through the valve: when $p \leq p$* there is an air mass entering the control volume, whereas if $p > p$* the air mass exhaustion happens.

On Fig. 3 is shown the valve force diagram, considering an unidiretional diaphragm deformation, and also that the forces F_{P_a} and F_p are uniformly distributed.

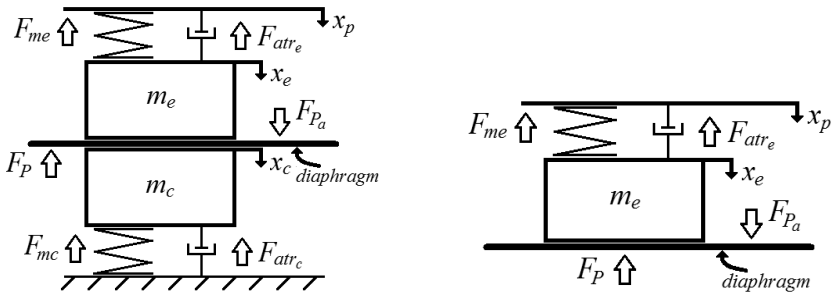

(a) For $p \leq p$* (b) For $p > p$*

Figure 3. Pressure valve force diagram.

Condition 1: for $p \leq p$*

At this condition, the force balance is given by Eq. 17:

$$m_{ec}\ddot{x}_{ec} = F_{me} + F_{P_a} - F_{atr_e} - F_{atr_c} - F_{mc} - F_P \tag{17}$$

where m_{ec} and x_{ec} are the plunger-spool set mass and displacement, respectively, F_{me} is the plunger spring force, F_{atr_e} is the plunger friction force, F_P is the force due to the air pressure into the control volume, F_{atr_c} is the spool friction force, F_{mc} is the spool spring force and F_{P_a} are the atmospheric pressure force.

The plunger spring force F_{me} and the spool spring force F_{mc} are given by:

$$F_{me} = k_{me}\left(x_p - x_{ec}\right) \tag{18}$$
$$F_{mc} = k_{mc} x_{ec} \tag{19}$$

where k_{me} and k_{mc} are the spring elasticity constants of the plunger and the spool, respectively, and x_p is the screw adjustment displacement.

ISSN 2176-5480

The friction forces F_{atr_e} and F_{atr_c} are considered only with their viscous component B_{me} and B_{mc}, being:

$$F_{atr_e} = B_{me}\dot{x}_{ec} \tag{20}$$

$$F_{atr_c} = B_{mc}\dot{x}_{ec} \tag{21}$$

The force due to the control volume pressure F_P is given by:

$$F_P = A_d p \tag{22}$$

where A_d is the diaphragm area.

Similarly, the force due to the atmospheric pressure F_{P_a} is:

$$F_{P_a} = A_d p_{atm} \tag{23}$$

Therefore, the force balance on the pressure valve for the condition when $p \leq p^*$ is given by:

$$\ddot{x}_{ec} = \frac{-\left(B_{me} + B_{mc}\right)\dot{x}_{ec} - \left(k_{me} + k_{mc}\right)x_{ec} + A_d\left(p_{atm} - p\right) + k_{me}x_p}{m_{ec}} \tag{24}$$

Condition 2: for $p > p^*$

Using the same analysis shown previously, the force balance for the condition when $p > p^*$ is:

$$\ddot{x}_e = \frac{-B_{me}\dot{x}_e - k_{me}x_e + A_d\left(p_{atm} - p\right) + k_{me}x_p}{m_e} \tag{25}$$

3.4 Linear model

The complete model of the pressure valve, taking into account only the linear range of the mass flow rate, is depicted by Eq. 8 and 24 — using also Eq. 15 — for the control volume pressurization condition, which are linear. For the exhausting condition, the mathematical model is depicted by Eq. 9 and 25 — using also Eq. 16 —, which is nonlinear due to the multiplication of two system states in Eq. 16, named x_e and p.

Using Taylor series for the system linearization, the equilibrium points for the condition $p > p^*$ are obtained considering $\dot{p} = \dot{x}_e = \ddot{x}_e = 0$. Assuming that the control volume equilibrium pressure is different than zero, it is obtained:

$$\begin{aligned} \overline{x}_e &= 0 \\ \overline{p} &= \frac{k_{me}}{A_d}\overline{x}_p. \end{aligned} \tag{26}$$

Hence, expanding Eq. 16 in Taylor series and neglecting the terms with order higher than one:

$$\begin{aligned} \overline{q}_e &= k_2 k_a \overline{p}\overline{x}_e = 0 \\ \mathbb{A} &= \left.\frac{\partial q_e}{\partial x_e}\right|_{p=\overline{p}} = k_2 k_a \overline{p} \\ \mathbb{B} &= \left.\frac{\partial q_e}{\partial p}\right|_{x_e=\overline{x}_e} = 0 \end{aligned}$$

Then, the linearized equation for the mass flow rate exhaustion q_e is given by,

$$\begin{aligned} q_e &\approx \overline{q}_e + \mathbb{A}\left(x_e - \overline{x}_e\right) + \mathbb{B}\left(p - \overline{p}\right) \\ &\approx k_2 k_a \overline{p} x_e \end{aligned} \tag{27}$$

Replacing Eq. 15 in Eq. 8 and converting it to Laplace complex frequency domain, the control volume dynamics for the pressurization condition ($p \leq p^*$) is depicted by:

$$\frac{P(s)}{X_p(s)} = \frac{c_1}{s^3 + c_2 s^2 + c_3 s + c_4} \tag{28}$$

where

$$c_1 = \frac{k_1 k_a k_{me} p_{sup} \gamma R T}{m_{ec} V} \quad c_2 = \frac{B_{me}+B_{mc}}{m_{ec}} \quad c_3 = \frac{k_{me}+k_{mc}}{m_{ec}} \quad c_4 = \frac{k_1 k_a A_d p_{sup} \gamma R T}{m_{ec} V}$$

Finally, replacing Eq. 27 in Eq. 9 and also converting it to Laplace domain, the linear control volume dynamics for the exhaustion condition ($p > p^*$) is given by:

$$\frac{P(s)}{X_p(s)} = \frac{c_5}{s^3 + c_6 s^2 + c_7 s + c_8} \tag{29}$$

being

$$c_5 = \frac{k_2 k_a k_{me} \overline{p} \gamma R T}{m_e V} \quad c_6 = \frac{B_{me}}{m_e} \quad c_7 = \frac{k_{me}}{m_e} \quad c_8 = \frac{k_2 k_a A_d \overline{p} \gamma R T}{m_e V}$$

ISSN 2176-5480

4. BLACK-BOX MODEL

This Section describes the black-box pressure valve identification using LS and PSO methods based on the valve mathematical model present in the previous Section, in order to obtain the internal valve parameters values.

Converting Eq. 28 and 29 to complex discrete time domain using Euler Method and considering the sampling input delay, the pressurization and exhaustion conditions are depicted respectively by:

$$\frac{P(z^{-1})}{X_p(z^{-1})} = \frac{b_0 z^{-1}}{1 + a_1 z^{-1} + a_2 z^{-2} + a_3 z^{-3}} \text{ for } p \leq p^* \tag{30}$$

$$\frac{P(z^{-1})}{X_p(z^{-1})} = \frac{b_1 z^{-1}}{1 + a_4 z^{-1} + a_5 z^{-2} + a_6 z^{-3}} \text{ for } p > p^* \tag{31}$$

being

$$\begin{array}{llll} b_0 = c_1 t_s^3 & a_1 = c_2 t_s - 3 & a_2 = c_3 t_s^2 - 2c_2 t_s + 3 & a_3 = c_4 t_s^3 - c_3 t_s^2 + c_2 t_s - 1 \\ b_1 = c_5 t_s^3 & a_4 = c_6 t_s - 3 & a_5 = c_7 t_s^2 - 2c_6 t_s + 3 & a_6 = c_8 t_s^3 - c_7 t_s^2 + c_6 t_s - 1 \end{array} \tag{32}$$

where t_s is the sampling time.

The experiments are carried out using a testbed composed by a manual pressure valve, a pressure sensor and a data acquisition system, consisted by an electronic board and computational software. In Tab. 1 is shown the main characteristics of the used devices, whereas Fig. 4 presents the tesbed schematic drawing.

Table 1. Testbed used devices.

Component	Brand	Part number
Manual pressure valve	Werk-Schott	3102-30
Pressure sensor	Sensata Technologies	100CP2-74
Data acquisition board	National Instruments	NI USB-6009

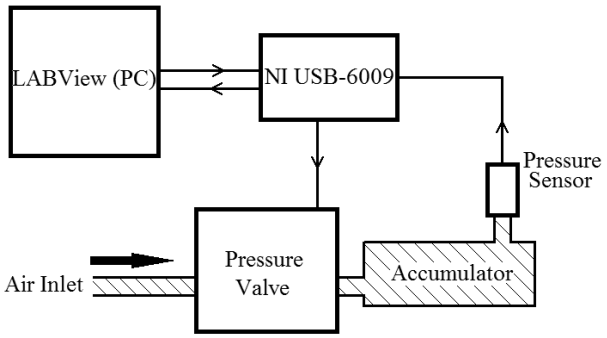

Figure 4. Testbed schematic drawing.

An initial step experiment is carried out in order to verify the acquisition system sampling time. Besides, previous experiments show that, one complete revolution in the valve knob displaces the adjustment screw in 1 mm. In addition, it is verified that a displacement $x_p = 1$ mm at this screw corresponds to a steady-state pressure of $1.56 \cdot 10^5$ Pa at valve oulet. Hence, a 0.25 mm step input is applied on the system at $t = 0$, considering a system previous manometric pressure of $0.895 \cdot 10^5$ Pa. The experiment result is shown on Fig. 5.

It is noted on Fig. 5 that the experimented curve may be approximated to a first order with transport delay system, so that its time constant τ is determined, neglecting the 0.1 s delay, as being $\tau = 0.15$ s, allowing the maximum board data acquisition time ($t_s = 0.005$ s).

Therefore, the system is submitted to the increasing and decreasing step experiment shown on Fig. 6, where it is noted the nonlinear valve behavior due to its hysteresis and dead band, which is about 0.9 mm. These features lead to a review on the mathematical valve model, since they are not predicted on Eq. 30 and 31. Hence, assuming only the valve linear behavior within the range cited in Section 3.2 ($0.894 \cdot 10^5$ Pa $\leq p \leq 3.224 \cdot 10^5$ Pa), it may be state that the system is depicted by a three different conditions piecewise model, being:

- if there is a positive screw displacement that is not within the valve dead band, Eq. 30 is considered;
- else if there is a negative screw displacement that is not within the valve dead band, Eq. 31 is considered;
- else the pressure stays steady.

ISSN 2176-5480

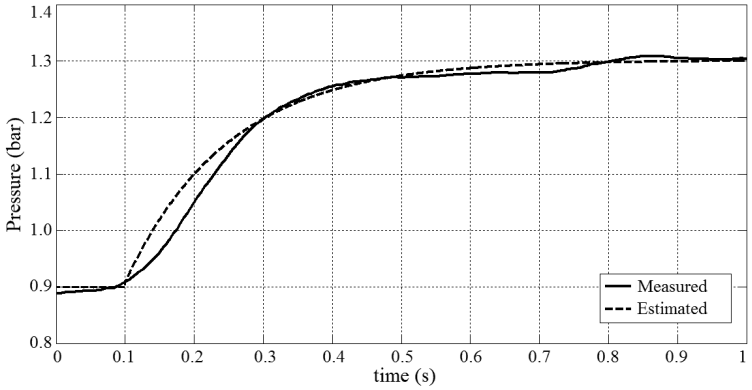

Figure 5. Pressure valve time constant.

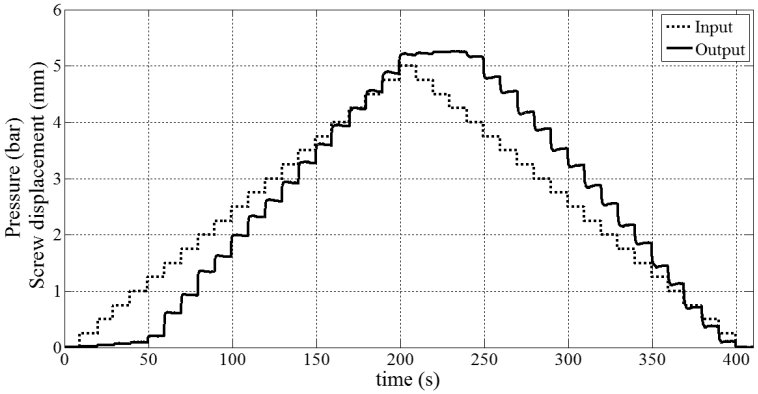

Figure 6. Step experiment.

Considering the cited linear pressure valve model, the parameter identification using Least Squares and Particle Swarm Optimization methods are presented in the following sections.

4.1 Least Squares identification

In many science fields, the linear system parameters determination is often carried out using Least Squares (LS) method, which was proposed by Karl Friedrich Gauss at the end of the 18th century.

The non-recursive LS method is used in offline batched analisys, or in other words, it is assumed that all the input and output data are available for the estimation algorithm. The estimated parameters vector $\hat{\mathbf{\Theta}}$ is given by (Ljung, 1987):

$$\hat{\mathbf{\Theta}} = \left[\mathbf{\Psi}^T \mathbf{\Psi}\right]^{-1} \mathbf{\Psi}^T \mathbf{Y}. \tag{33}$$

where $\mathbf{\Psi}$ is the regressors matrix and $\mathbf{Y}$ is the experimental output data vector, which in this paper are given by,

$$\mathbf{\Psi} = \begin{bmatrix} -p(k-1) & -p(k-2) & -p(k-3) & x_p(k-1) \\ \vdots & \vdots & \vdots & \vdots \\ -p(N-1) & -p(N-2) & -p(N-3) & x_p(N-1) \end{bmatrix} \quad \mathbf{Y} = \begin{bmatrix} p(k) \\ \vdots \\ p(N) \end{bmatrix}$$

being k the discrete time and N the experimented data number. It is important to notice that, in order to better fit the experimented and estimated parameters, the input and output vector are considered with zero mean.

Two different parameters estimation are performed, according to the linear valve conditions presented in Eq. 30 and 31. For the cited conditions, the identified parameters using LS method are:

$$\begin{array}{llll} b_0 = 117420.7 & a_1 = -1.3735 & a_2 = -0.1457 & a_3 = 0.5200 \\ b_1 = 199160.3 & a_4 = -1.2985 & a_5 = -0.1678 & a_6 = 0.4677 \end{array} \tag{34}$$

4.2 Particle Swarm Optimization identification

Particle Swarm Optimization (PSO) is a stochastic optimization technique first presented by Kennedy and Eberhart (1995). The algorithm is based on the behaviour of bird flocking and fich schooling. The main PSO idea is similar to other evolutionary computation techniques as Genetic Algorithms (GA).

ISSN 2176-5480

Since its begin, the application of PSO has increased in many fields beyond engineering, such as psychology (Kennedy, 1997), product design (Yildiz, 2009), economy (Moraes and Nagano, 2012) and even in musicology (Blackwell and Bentley, 2002).

The increase on PSO related research are justified due to its faster and cheaper convergence compared to other methods when applied on nonlinear systems, besides having only few adjustment parameters (Valdez and Melin, 2007).

The concept of the optimization consists of updating the particle position and speed towards its best solution. Each particle is updated using its own best found position and the global swarm best position, which makes the convergence to the final solution faster. It is easily demonstrated by the following equations, which correspond to the *canonical* PSO introduced by Clerc and Kennedy (2002):

$$\boldsymbol{v}_i^{t+1} = \chi\left[\boldsymbol{v}_i^t + \varphi_1 \boldsymbol{U}_1(0,1) * \left(\boldsymbol{p}_i - \boldsymbol{x}_i^t\right) + \varphi_2 \boldsymbol{U}_2(0,1) * \left(\boldsymbol{s} - \boldsymbol{x}_i^t\right)\right] \tag{35}$$

$$\boldsymbol{x}_i^{t+1} = \boldsymbol{x}_i^t + \boldsymbol{v}_i^{t+1} \tag{36}$$

being the *constriction factor* χ given by,

$$\chi = \frac{2k}{\left|2 - \varphi - \sqrt{\varphi^2 - 4\varphi}\right|} \tag{37}$$

where $\boldsymbol{v}_i^t$ and $\boldsymbol{x}_i^t$ are the speed and position of the particle i, respectively, $\boldsymbol{p}_i$ is the own best particle solution, $\boldsymbol{s}$ is the best swarm solution, φ_1 and φ_2 are constants called *cognitive* and *social* acceleration coefficients, $\boldsymbol{U}_1(0,1)$ and $\boldsymbol{U}_2(0,1)$ are random values $\in [0,1]$, $*$ is an element-by-element vector multiplication operator, k is an arbitrary coefficient usually set to 1 and $\varphi = \varphi_1 + \varphi_2$, being usually $\varphi_1 = \varphi_2 = 2.05$ (Eberhart and Shi, 2000).

Therefore, using Eq. 35 and 36 to identify the pressure valve parameters and considering the two different conditions ($p \leq p^*$ and $p > p^*$), the PSO algorithm gives:

$$\begin{array}{llll} b_0 = 421310.6 & a_1 = -1.3733 & a_2 = -0.1456 & a_3 = 0.5219 \\ b_1 = 311826.7 & a_4 = -1.2977 & a_5 = -0.1677 & a_6 = 0.4677 \end{array} \tag{38}$$

5. INTERNAL PARAMETER DETERMINATION

The identification of the empirical parameters shown in the previous sections allows the internal pressure valve unknown constant determination.

Solving the linear system composed by the equations shown in (32) using the identified values presented in (34) and (38) in addition with Eq. 26 and considering the viscous friction components $B_{me} = B_{mc} = 12$ Ns/m according to Carducci *et al.* (2006), the identified valve parameters are presented in Tab. 2. The system constants are shown in Tab. 3.

Table 2. Identified internal pressure valve parameters.

Parameter [Unity]	LS	PSO
A_d [m^2]	$17.77 \cdot 10^{-3}$	$18.57 \cdot 10^{-3}$
m_e [kg]	$17.30 \cdot 10^{-3}$	$17.30 \cdot 10^{-3}$
m_c [kg]	$16.79 \cdot 10^{-3}$	$16.77 \cdot 10^{-3}$
k_{me} [N/m]	2607.56	2607.63
k_{mc} [N/m]	2702.85	2705.23
k_1 [m]	$8.2 \cdot 10^{-9}$	$29.4 \cdot 10^{-9}$
k_2 [m]	$14.3 \cdot 10^{-6}$	$23.4 \cdot 10^{-6}$

Table 3. System constants.

Parameter	Value [Unity]	Parameter	Value [Unity]
γ	1.4 [1]	R	287.04 [J/(K· kg)]
T	298 [K]	V	$149.74 \cdot 10^{-6}$ [m^3]
p_{sup}	$8 \cdot 10^5$ [Pa]	k_a	$2.34 \cdot 10^{-3}$ [s/m]
B_{me}	12 [Ns/m]	B_{mc}	12 [Ns/m]
$\overline{x}_p$	$2.69 \cdot 10^{-3}$ [m]	t_s	0.005 [s]

On Fig. 7 and 8 are shown the system simulation using the experimented parameters obtained with LS and PSO methods, considering only the valve linear behavior range ($0.894 \cdot 10^5$ Pa $\leq p \leq 3.224 \cdot 10^5$ Pa).

ISSN 2176-5480

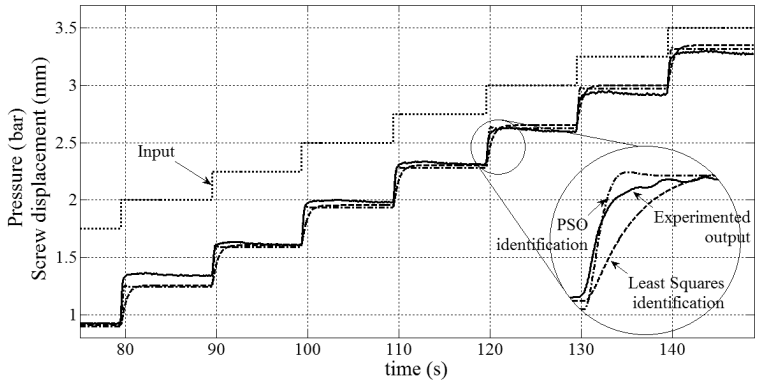

Figure 7. Validation for system pressurization.

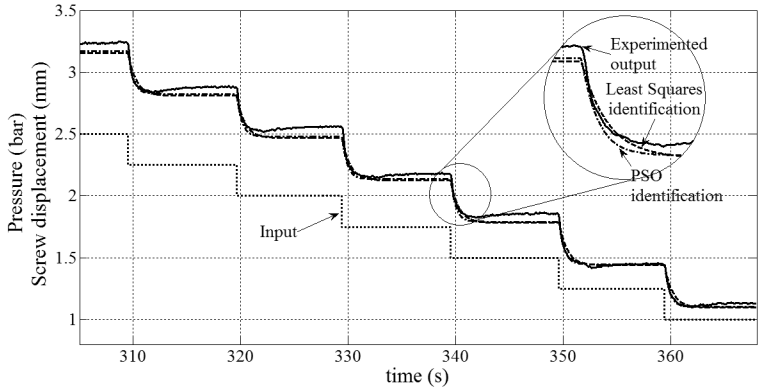

Figure 8. Validation for system exhaustion.

In order to evaluate and compare the both used identification methods, the fitting coefficient shown in Eq. 39 is used, being y, $\hat{y}$ and $\overline{y}$ the measured, the estimated and the mean value of the measured output, respectively.

$$\text{fit} = 100 \cdot \left(1 - \frac{||\hat{y} - y||}{||y - \overline{y}||}\right) \tag{39}$$

Finally, using Eq. 39, it is stated that, considering the used pressure valve linear behavior range, it is shown in Tab. 4 the reached accuracy using LS and PSO identification methods concerning to the experimented pressurization and exhaustion values.

Table 4. LS and PSO accuracy.

System Condition	LS	PSO
Pressurization	90.54%	92.48%
Exhaustion	91.79%	93.11%

6. CONCLUSIONS

It is well known that pneumatics plays an important role when alternative ways to control mechanical systems are discussed. However, the intrinsic problems concerned to pneumatics — mainly due to friction, air compressibility and unknown valve internal parameters — complicate its modeling and control design.

Therefore, this paper proposes a systematic way to address the third cited problem. The internal parameters identification of a pneumatic manual pressure valve within its linear range behavior is carried out using Mass and Energy Conservation Theory in conjunction with empirical experiments. The valve empirical model order is based on its mathematical model order, so that the identification is performed directly.

In order to check two different methods of system identification, Least Squares (LS) and Particle Swarm Optimization (PSO) are used. At last, it is shown that the identification carried out with PSO present better results than the ones with LS, although both results are able to depict the valve dynamics with more than 90% of accuracy.

The obtained results state that a linear identification method is not able to produce the better fitting result for the proposed system, even when considering only the linear valve operating range. This is mainly due to the compressed air

ISSN 2176-5480

nonlinear feature. Therefore, further studies will investigate the full range identification of the used pressure valve through nonlinear methods, such as PSO.

7. REFERENCES

Ali, H.I., Bahari, S., Noor, B.M., Bashi, S.M. and Marhaban, M.H., 2009. "A review of pneumatic actuators (Modeling and Control)". *Australian Journal of Basic and Applied Sciences*, Vol. 3, No. 2, pp. 440–454.

Barreto, F., 2003. *Modelagem e controle não-lineares de um posicionador servopneumático industrial*. Master's thesis, Universidade Federal de Santa Catarina.

Blackwell, T.M. and Bentley, P., 2002. "Improvised music with swarms". In *Proceedings of the 2002 Congress on Evolutionary Computation - CEC 2002*. Vol. 2, pp. 1462–1467.

Carducci, G., Giannoccaro, N.I., Messina, A. and Rollo, G., 2006. "Identification of viscous friction coefficients for a pneumatic system model using optimization methods". *Mathematics and Computers in Simulation*, Vol. 71, No. 71, pp. 385 – 394. ISSN 0378-4754.

Carneiro, J.F. and Almeida, F.G., 2006. "Modeling pneumatic servovalves using neural networks". In *Computer Aided Control System Design, 2006 IEEE International Conference on Control Applications, 2006 IEEE International Symposium on Intelligent Control, 2006 IEEE*. Munique, DE, pp. 790 –795.

Carneiro, J.F. and Almeida, F.G., 2011. "Undesired oscillations in pneumatic systems". In *Nonlinear Science and Complexity*, Springer Netherlands, pp. 229–243.

Clerc, M. and Kennedy, J., 2002. "The particle swarm - explosion, stability, and convergence in a multidimensional complex space". *IEEE Transactions on Evolutionary Computation*, Vol. 6, pp. 58 – 73.

Curatolo, D., Hoffmann, M. and Stein, B., 2003. "Hilfe von FluidSIM".

Dall'Amico, R., 2011. "Fundamentos da Pneumática II".

Eberhart, R. and Shi, Y., 2000. "Comparing inertia weights and constriction factors in particle swarm optimization". In *Proceedings of the 2000 IEEE Congress on Evolutionary Computation*. IEEE Press, Piscataway, USA, pp. 84 – 88.

Festo, 2010. *Servopneumatics*.

Fox, R.W. and McDonald, A.T., 1985. *Introduction to Fluid Mechanics*. Wiley.

Guenther, R. and Perondi, E.A., 2004. "O controle em cascata de um sistema pneumático de posicionamento". *Revista Controle & Automação*, Vol. 15, pp. 149–161.

Kennedy, J., 1997. "The particle swarm: social adaptation of knowledge". In *Evolutionary Computation, 1997., IEEE International Conference on*. pp. 303–308.

Kennedy, J. and Eberhart, R., 1995. "Particle swarm optimization". In *Proceedings of IEEE International Conference on Neural Networks*. IEEE Press, Piscataway, USA, pp. 1942 – 1948.

Ljung, L., 1987. *System identification: theory for the user*. Prentice-Hall information and system sciences series. Prentice-Hall. ISBN 9780138816407.

Moraes, M.B.C. and Nagano, M.S., 2012. "Cash balance management: A comparison between genetic algorithms and particle swarm optimization". *Acta Scientiarum. Technology*, Vol. 34, No. 4, pp. 373 – 379.

Perondi, E., 2002. *Controle não-linear em cascata de um servoposicionador pneumático com compensação do atrito*. Ph.D. thesis, Universidade Federal de Santa Catarina - UFSC.

Ritter, C.S., 2010. *Modelagem Matemática das Características Não-Lineares de Atuadores Pneumáticos*. Master's thesis, Universidade Regional do Nordeste do Estado do Rio Grande do Sul - UNIJUÍ.

Scholz, D. and Zimmermann, A., 1993. *Pneumatic NC Axes*, Vol. 1. Festo Didactic KG, Esslingen, DE.

Sorli, M., Figliolini, G. and Pastorelli, S., 2001. "Dynamic model of a pneumatic proportional pressure valve". In *Advanced Intelligent Mechatronics, 2001. Proceedings. 2001 IEEE/ASME International Conference on*. Vol. 1, pp. 630 – 635.

Taghizadeh, M., Ghaffari, A. and Najafi, F., 2009. "Modeling and identification of a solenoid valve for PWM control applications". *Comptes Rendus Mécanique*, Vol. 337, pp. 131–140.

Valdez, F. and Melin, P., 2007. "Parallel evolutionary computing using a cluster for mathematical function optimization". In *Fuzzy Information Processing Society, 2007. NAFIPS '07. Annual Meeting of the North American*. pp. 598–603.

Yildiz, A.R., 2009. "A novel particle swarm optimization approach for product design and manufacturing". *The International Journal of Advanced Manufacturing Technology*, Vol. 40, pp. 617 – 628.

8. RESPONSIBILITY NOTICE

The authors are the only responsible for the printed material included in this paper.